Reconsideration of the Source Model for the 1662 Hyuga-nada Earthquake

Yusuke Yamashita (yamac@rcep.dpri.kyoto-u.ac.jp)
Kyoto Daigaku https://orcid.org/0000-0002-5347-5216
Kei Ioki
Sangyo Gijutsu Sogo Kenkyujo
Yoshihiro Kase
Hokkaido Research Organization

Express Letter

Keywords: Hyuga-nada earthquake, Tsunami, Slow earthquake, Historical earthquake

Posted Date: July 2nd, 2020

DOI: https://doi.org/10.21203/rs.3.rs-38243/v1

Title page:

Title:

Reconsideration of the source model for the 1662 Hyuga-nada Earthquake

Author #1(Corresponding author): Yusuke Yamashita, Miyazaki Observatory, Research Center for Earthquake Prediction, Disaster Prevention Research Institute, Kyoto University, 3884 Kaeda, Miyazaki 889-2161, Japan, yamac@rcep.dpri.kyoto-u.ac.jp

Author #2: Kei Ioki, Geological Survey of Japan, National Institute of Advanced Industrial Science and Technology, Central 7, 1-1-1 Higashi, Tsukuba, Ibaraki 305-8567, Japan., kei-ioki@aist.go.jp

Author #3: Yoshihiro Kase, Geological Survey of Hokkaido, Hokkaido Research Organization, Kita 19-jyo Nishi 12-chome, Kita-ku, Sapporo, Hokkaido 060-0819, Japan, kase-yoshihiro@hro.or.jp

Indicate the corresponding author:

Yusuke Yamashita

Abstract

The 1662 Hyuga-nada Earthquake is one of the largest earthquakes to have occurred in the Hyuga-nada region, Southwest Japan, rupturing the western part of the Nankai Trough subduction zone. Strong ground motion and a large tsunami with an estimated height of at least 4–5 m were reported along the coast of Miyazaki Prefecture, Kyushu Island, with extensive damage reported across this region. Therefore, developing a more complete picture of the 1662 Hyuga-nada Earthquake will improve our understanding of tsunami risk along the Pacific coast of Southwest Japan. Here we use the most recent geophysical data from the region to propose a novel source model for the 1662 Hyuga-nada Earthquake that incorporates our current understanding of the interactions between slow earthquakes and great earthquakes. The source area in our proposed model extends from the focal region of recurrent M7-class interplate earthquakes to the region of slow earthquakes that occur at relatively shallow depths along the plate boundary. Tsunami simulations indicate that the predicted coastal tsunami heights are broadly compatible with previously reported tsunami heights. This new model suggests that the 1662 Hyuga-nada Earthquake was probably a M8-class earthquake, and that

33 previous magnitude determinations may have underestimated the strength of this
34 historic earthquake. However, the model uncertainty remains large, and the calculated
35 tsunami heights for the southern coast of Miyazaki Prefecture are very high. We suggest
36 that future verification, including an analysis of tsunami-related deposits along the coast,
37 will be important to more accurately determine the source area of the 1662 Hyuga-nada
38 Earthquake.
39

40 **Keywords**

41 Hyuga-nada earthquake; Tsunami; Slow earthquake; Historical earthquake

Main Text

1. Introduction

Hyuga-nada is located in the western part of the Nankai Trough, Southwest Japan, in a seismically active region where M7-class subduction zone earthquakes have occurred at regular intervals during the last 100 years (Fig. 1). The earthquake focal regions are relatively close to the coastline, and significant damage has been caused by strong ground motion and tsunami. The largest historical earthquake in this area is the 1662 M 7.6 Hyuga-nada Earthquake, which resulted in many deaths in the coastal areas of Miyazaki Prefecture (Usami, 2003; Utsu, 1999; Headquarters for Earthquake Research Promotion, 2004). The 1662 Hyuga-nada Earthquake has been characterized by strong ground motion and a tsunami with an estimated height of 4–5 m in the coastal areas around Miyazaki Plain (Hatori, 1985; Tsuji et al., 2018) that cannot be attributed to earthquakes that have occurred in the last 100 years. The source location and rupture process of this earthquake is still unclear due to limited historical information and a paucity of geological studies on tsunami-related coastal sediments. However, given the possibility that a similar magnitude earthquake will occur in the Hyuga-nada

region in the future, a better understanding of the 1662 Hyuga-nada Earthquake is vital for disaster management and tsunami modeling in the coastal areas stretching from Kyushu to Shikoku.

Recent geophysical data have been used to investigate the interactions between great earthquakes and slow earthquakes (e.g., Obara and Kato, 2016). For example, Ito et al. (2013) documented a spatio-temporal relationship between the large coseismic slip area of the 2011 M_w 9.0 Tohoku Earthquake and a shallow slow slip event (SSE) that started one month prior to the Tohoku mainshock. This important observation shows that the coseismic slip region of a great earthquake and focal region of shallow slow slip can coexist on the same plate boundary. The shallow SSE also occurred in the same region in 2008, and appears to have occurred repeatedly in the past (Uchida et al., 2016). A similar relationship has been reported for the 2014 M_w 8.1 Iquique Earthquake, Northern Chile (Ruiz et al., 2014). Wallace et al. (2016) also suggested a relationship between a shallow SSE and tsunamigenic earthquakes along the northern Hikurangi subduction zone, New Zealand, where seafloor observations showed that slip during the shallow SSE reached the trench axis and partly overlapped with the epicentral areas of

74 past tsunamigenic earthquakes.

75 Conversely, the focal regions of shallow slow earthquakes are often considered to
76 possess velocity-strengthening frictional properties that do not allow fast ruptures to
77 nucleate spontaneously. For example, the focal regions of a shallow SSE acted as
78 barriers to seismic rupture propagation during the 2012 M_w 7.6 Costa Rica (Dixon et al.,
79 2014) and 2016 M_w 7.6 Ecuador (Rolandone et al., 2018) earthquakes. A similar spatial
80 relationship was also reported for the focal region of the 2011 Tohoku Earthquake in the
81 Japan Trench (Nishikawa et al., 2019).

82 The abovementioned results appear to be contradictory with regard to the slip
83 behavior in the focal regions of shallow slow earthquakes. However, the results from
84 laboratory friction experiments using samples recovered from scientific drilling after the
85 2011 Tohoku Earthquake (Ito et al., 2017) show that an increase in sliding velocity can
86 promote a change from steady-state or slip-strengthening frictional behavior to
87 slip-weakening frictional behavior. This indicates that the slip behavior within the focal
88 region of a shallow slow earthquake can change depending on whether slip is ongoing
89 or not, or whether the slip velocity becomes slightly higher than that during discrete

90 SSEs (Ito et al., 2017). The means that ongoing slow earthquake slip may reduce the
91 fault strength and promote the propagation of fault rupture during the mainshock,
92 thereby increasing the earthquake magnitude.

93 Here we use the latest geophysical findings on the relationships between recent
94 large earthquakes and shallow slow earthquakes to reconsider the fault source model for
95 the 1662 Hyuga-nada Earthquake, and then discuss this new model in the context of
96 previous studies.

97

98 **2. Slip characteristics of the plate boundary in the Hyuga-nada region**

99 While there is an absence of seismicity related to ordinary earthquakes in the
100 shallow part of the plate boundary in the Hyuga-nada region, slow earthquakes are very
101 active in this region. Shallow very-low-frequency earthquakes (e.g., Asano et al., 2015;
102 Obara and Ito, 2005) and low-frequency tremor (Yamashita et al., 2015) are activated
103 once every few years in the Hyuga-nada region, and exhibit characteristic migration
104 patterns that are indicative of episodic SSEs on the shallow plate boundary. The focal
105 regions of M7-class interplate earthquakes, which are thought to repeat every few

106 decades, are located on the down-dip side of the shallow slow earthquake source
107 regions (Yagi et al., 1999)(Fig. 1). Microearthquakes, including small repeating
108 earthquakes (Igarashi, 2010; Yamashita et al., 2012), are also common in this region.

109 The slip phenomena in the Hyuga-nada region show many similarities to the plate
110 boundary in Miyagi Prefecture prior to the 2011 Tohoku Earthquake, including a
111 relatively shallow focal region of slow earthquakes (e.g., Ito et al., 2013; Katakami et al.,
112 2018), a co-seismic slip area located on the down-dip side of the slow earthquake region
113 (Miyagi-Oki earthquake; (Yamanaka and Kikuchi, 2004), and frequent microseismicity,
114 including small repetitive earthquakes (e.g., Igarashi et al., 2003; Uchida and
115 Matsuzawa, 2013). It is possible that an earthquake with similar characteristics to the
116 2011 Tohoku Earthquake may occur in the Hyuga-nada region in the future since the
117 Hyuga-nada and Miyagi regions are located above different subducting plates.

118

119 **3. Revised fault model for the 1662 Hyuga-nada Earthquake**

120 Although it is unknown whether slip behavior similar to that in the Miyagi region
121 may occur along the plate boundary in the Hyuga-nada region, our revised fault model

122 for the 1662 Hyuga-nada Earthquake adopts similar mechanisms to those of the 2011
123 Tohoku Earthquake. Specifically, the model involves coseismic rupture extending
124 between the focal regions of M7-class earthquakes and shallow slow earthquakes (Figs.
125 2a and b). When considering the fault location, we assume that the focal region is
126 located in the southern part of the Hyuga-nada region based on the distribution of
127 damage described in historical records. Strong ground motion is mainly generated in the
128 focal region of M7-class interplate earthquakes that occur every few decades on the
129 down-dip side of the plate boundary, and large tsunami are generated from the focal
130 region of the shallow slow earthquakes.

131 It is also necessary to consider the influence of Kyushu-Palau Ridge (KPR) as it
132 subducts under the Hyuga-nada region (e.g., Yamamoto et al., 2013) because this will
133 determine how far the rupture can spread along the shallow plate boundary. Stress can
134 concentrate on the down-dip side of subducting seamounts (e.g., Mochizuki et al., 2008),
135 which results in unfavorable conditions for the generation and propagation of large
136 ruptures (e.g., Wang and Bilek, 2014). Other observations have indicated that the
137 migration of shallow low-frequency tremor and slip propagation during shallow SSEs

138 can be inhibited by subducting seamounts (Wallace et al., 2016; Yamashita et al., 2015).
139 Therefore, our model assumes that fault rupture along the shallow plate boundary does
140 not reach the trench axis, as was experienced during the Tohoku earthquake, but only
141 extends as far as the region where the migration path of the shallow slow earthquakes
142 changes due to the influence of KPR (Fig. 2a). The parameters of each subfault in the
143 model are summarized in Table 1. The depth and dip angles of the subfaults were
144 determined using a plate boundary model (Nakanishi et al., 2018) that was obtained by
145 compiling the structural data from offshore surveys. The slip amount in the model,
146 which was determined by a trial-and-error process during the tsunami simulations, was
147 set to be larger at shallower depths. The total seismic moment was calculated to be 9.60
148 $\times 10^{20}$ Nm (M_w 7.9) when the modulus of rigidity was 3.43×10^{10} N/m^2.
149

150 **4. Tsunami simulation for the 1662 Hyuga-nada Earthquake based on the new**
151 **fault model**

152 We simulated the tsunami using the “iRIC” (International River Interface
153 Cooperative) numerical simulation platform and its "ELIMO" (Easy-performable

154 Long-wave Inundation MOdel) solver to verify whether the tsunami predicted by the
155 new fault model was compatible with historical reports. The bathymetric data were
156 sourced from the GEBCO_2014 one-minute mesh data that were provided by the
157 British Oceanographic Data Center. The initial vertical deformation of the seafloor due
158 to coseismic slip was calculated using the formulas outlined in Okada (1992) and
159 Tanioka and Satake (1996). We assumed that the initial displacement of the sea surface
160 was equal to the initial vertical deformation of the seafloor. The non-linear long-wave
161 equations were solved using third-order finite difference computations. A 0.01-degree
162 grid spacing (latitude and longitude) was used in the simulations.

163 Figure 2a shows the revised fault model developed in this study, as well as the
164 predicted and measured tsunami heights along the coastal areas of Miyazaki Prefecture.
165 The source fault is divided into northern and southern segments, with the results of
166 calculations using only the northern segment shown in Fig. 2b to verify the contribution
167 from the southern segment. Note that the points used to calculate the tsunami heights
168 are the nearest offshore grid points from the onshore areas of interest, such that the
169 calculations are not equivalent to the tsunami inundation simulations. The tsunami

170 heights calculated from our proposed model (Fig. 2a) are broadly consistent with the
171 inundation and runup heights reported by Hatori (1985) and Tsuji et al. (2018), which
172 are indicated by the red and gray circles, respectively, in Fig. 2. We believe that rupture
173 of the southern fault segment is required to explain the observed tsunami characteristics
174 in the southern part of Miyazaki Plain based on the results in Fig. 2b.
175
176 **5. Discussion**
177 Fault models for the 1662 Hyuga-nada Earthquake have previously been proposed
178 by Hatori (1985) and Matsu'ura et al. (2003) (hereafter the Hatori model and Matsu'ura
179 model, respectively). We also examined whether these two models can explain the
180 tsunami heights reported in previous studies (Figs. 2c and d). We assumed a rectangular
181 source fault in the calculations, even though the source regions in the previous fault
182 models were elliptical in shape, and source parameters, such as the slip amount, were
183 not reported. The source region in the Hatori model extends below the eastern coastline
184 of Kyushu, and the depth to the plate boundary at the base of the model is
185 approximately 40 km (Fig. 2c). More than 10 m of slip is required to generate an

186 ~5-m-high tsunami in the coastal area of Miyazaki Plain, which would equate to a M_w
187 8.0 or greater earthquake (Fig. 2c is the case of 10 m of slip), when we assume that the
188 Hatori model involves an interplate earthquake. The afterslip events related to the
189 October 1996 (M_J 6.9) and December 1996 (M_J 6.7) earthquakes slightly overlap in the
190 source region of the Hatori model (Yagi et al., 2001), and deep long-term SSEs
191 (L-SSEs) (M_w 6–7) occur once every few years (Ozawa, 2017; Takagi et al., 2019; Yarai
192 and Ozawa, 2013). Takagi et al. (2019) estimated that there was significantly more slip
193 in the source region of the Hatori model, which is considered to be a stable region for
194 slow fault slip rather than fast slip, via analysis of the cumulative slip distribution of
195 deep L-SSEs that occurred in the last 20 years. Furthermore, static crustal deformation
196 with 1+ m of uplift would be expected in Miyazaki Plain, but there are no reports of
197 such uplift due to the 1662 Hyuga-nada Earthquake. These factors suggest that the
198 Hatori model may be an unrealistic fault model for the 1662 Hyuga-nada Earthquake.
199 The Matsu'ura model (Fig. 2d) is based on the seismic intensity distribution
200 estimated from historical records of the 1662 Hyuga-nada Earthquake. The location of
201 the source region was estimated via a comparison with past earthquakes that possessed

202 reliable seismic intensity observations. Although the source region partially overlaps
203 with the fault model in this study, the 1662 Hyuga-nada Earthquake is estimated to be a
204 M 7.2–7.5 event in the Matsu'ura model. Even if we assume M_w 7.5 (equivalent to a
205 fault slip of 5 m), the maximum tsunami height in the southern part of Miyazaki Plain is
206 about 2.5 m using the Matsu'ura model (Fig. 2d), which is much smaller than the
207 observed tsunami heights of about 4–5 m. Fault slip at relatively shallow depths along
208 the plate boundary generally contributes significantly to tsunami generation, but it is
209 less important in generating strong ground motion. Therefore, the fault size and
210 earthquake magnitude based on seismic intensity tend to be underestimated when the
211 source region is relatively shallow.

212 An inlet was formed in the Kibana area of Miyazaki Plain after the 1662 Hyuga-nada
213 Earthquake due to subsidence. Our proposed fault model predicts several tens of
214 centimeters of subsidence in Miyazaki Plain. Niwa et al. (2020) acquired sediment cores
215 in this area and found a sedimentary horizon containing marine sediments about 2 m
216 below the present surface, suggesting that this horizon may have formed in a temporary
217 marine inlet after the 1662 Hyuga-nada Earthquake. This temporarily submerged area

218 was subsequently used as rice fields, with up to 2 m of subsidence only documented
219 locally on maps that were made after the earthquake. Assuming that the 1662
220 Hyuga-nada earthquake was an interplate earthquake, these observations of up to 2 m of
221 subsidence suggest that liquefaction due to strong ground motion, as opposed to static
222 crustal deformation due to the earthquake, was the main driver of subsidence.

223 Our proposed fault model appears to be the most suitable among the four tsunami
224 simulation models to explain the observed inundation and runup heights (Fig. 2e). Our
225 results suggest that the magnitude of the 1662 Hyuga-nada Earthquake is comparable to
226 a M8-class earthquake, and that previous studies may have underestimated the
227 magnitude of this earthquake. However, it is difficult to definitively validate the fault
228 models due to the limited amount of historical information concerning the 1662
229 Hyuga-nada Earthquake. Our proposed fault model appears to be the most suitable at
230 present to explain some of the characteristics of the 1662 Hyuga-nada Earthquake,
231 although other models may also be compatible with the tsunami heights reported in
232 previous studies.

233 Shrines in Miyazaki Prefecture that retain descriptions and stories of the 1662

234 Hyuga-nada Earthquake may be a useful source of information to complement an
235 analysis of tsunami-related deposits. However, while our fault model predicts a large
236 tsunami along the northern parts of the Nichinan coastal area (Fig. 2e), there is currently
237 no historical or scientific evidence to evaluate this prediction. Therefore, it will be
238 necessary to conduct more extensive surveys of tsunami deposits and historical records,
239 and verify these using tsunami inundation simulations, such as those used to investigate
240 the 17th century great earthquake off Hokkaido (Ioki and Tanioka, 2016), to construct a
241 more detailed source model for the 1662 Hyuga-nada Earthquake.
242
243 **6. Conclusion**
244 We proposed a new fault model for the 1662 Hyuga-nada Earthquake that was based
245 on a modern geophysical understanding of the relationships between great earthquakes
246 and shallow slow earthquakes, whereby coseismic slip extends into the shallow focal
247 region of active slow earthquakes. Our results suggest that this earthquake may have
248 been a M8-class earthquake since the simulated tsunami heights are generally consistent
249 with those reported in previous studies. However, there are substantial uncertainties in

250 the model, such that it will be necessary to validate the model predictions by conducting
251 surveys of coastal tsunami deposits and investigating historical documents, and then
252 performing new tsunami inundation simulations with these new data.
253

254 Declarations

255 Ethics approval and consent to participate

256 Not applicable

257 Consent for publication

258 Not applicable

259 List of abbreviations

260 M_J: Japan Meteorological Agency magnitude

261 M_W: Moment magnitude

262 PHS: Philippine Sea Plate

263 EU: Eurasian Plate

264 KPR: Kyushu-Palau Ridge

265 SSE: Slow slip event

L-SSE: Long-term slow slip event

Availability of data and materials

The iRIC software (including solver ELIMO) can be downloaded from https://i-ric.org/.

Competing interests

The authors declare that they have no competing interests.

Funding

This research was supported by JSPS Research Grants 16H06473 and 17K01328.

Authors' contributions

YY designed the study, performed the tsunami simulations, and wrote the manuscript. KI supported the tsunami simulations and geophysical interpretations. YK supported the geological interpretations. All of the authors read and approved the final manuscript.

Acknowledgements

We performed tsunami simulations using the ELIMO solver (https://i-ric.org/solvers/elimo/) from iRIC (https://i-ric.org/); ELIMO was developed by Professor Yasunori Watanabe at Hokkaido University. We gratefully appreciate insightful discussions with Professor Yoshihiro Ito on the interaction between slow and fast earthquakes. The figures were created using the Generic Mapping Tools software (Wessel and Smith, 1998). This research was supported by JSPS Research Grants 16H06473 and 17K01328.

290 **References**

291 Asano Y, Obara K, Matsuzawa T, Hirose H, Ito Y (2015) Possible shallow slow slip
292 events in Hyuga-nada, Nankai subduction zone, inferred from migration of very low
293 frequency earthquakes. Geophys Res Lett 42 (2):331-338. doi:10.1002/2014gl062165

294 Dixon TH, Jiang Y, Malservisi R, McCaffrey R, Voss N, Protti M, Gonzalez V (2014)
295 Earthquake and tsunami forecasts: relation of slow slip events to subsequent earthquake
296 rupture. Proc Natl Acad Sci USA 111 (48):17039-17044. doi:10.1073/pnas.1412299111

297 Hatori T (1985) Field investigation of historical tsunamis along the east coast of Kyushu,
298 West Japan. Bull Earthquake Res Inst Univ Tokyo 60:439-459

299 Headquarters for Earthquake Research Promotion (2004) Long-term evaluation of
300 seismicity off Hyuga and Southwestern Islands areas along Ryukyu trench.

301 Igarashi T (2010) Spatial changes of inter-plate coupling inferred from sequences of
302 small repeating earthquakes in Japan. Geophys Res Lett 37 (20):L20304.
303 doi:10.1029/2010gl044609

304 Igarashi T, Matsuzawa T, Hasegawa A (2003) Repeating earthquakes and interplate

305 aseismic slip in the northeastern Japan subduction zone. J Geophys Res 108 (B5):2249.
306 doi:10.1029/2002jb001920

307 Ioki K, Tanioka Y (2016) Re-estimated fault model of the 17th century great earthquake
308 off Hokkaido using tsunami deposit data. Earth Planet Sci Lett 433:133-138.
309 doi:10.1016/j.epsl.2015.10.009

310 Ito Y, Hino R, Kido M, Fujimoto H, Osada Y, Inazu D, Ohta Y, Iinuma T, Ohzono M,
311 Miura S, Mishina M, Suzuki K, Tsuji T, Ashi J (2013) Episodic slow slip events in the
312 Japan subduction zone before the 2011 Tohoku-Oki earthquake. Tectonophysics
313 600:14-26. doi:10.1016/j.tecto.2012.08.022

314 Ito Y, Ikari MJ, Ujiie K, Kopf A (2017) Coseismic slip propagation on the Tohoku plate
315 boundary fault facilitated by slip-dependent weakening during slow fault slip. Geophys
316 Res Lett 44 (17):8749-8756. doi:10.1002/2017gl074307

317 Katakami S, Ito Y, Ohta K, Hino R, Suzuki S, Shinohara M (2018) Spatiotemporal
318 Variation of Tectonic Tremor Activity Before the Tohoku-Oki Earthquake. J Geophys
319 Res 123 (11):9676-9688. doi:10.1029/2018jb016651

320 Kreemer C, Blewitt G, Klein EC (2014) A geodetic plate motion and Global Strain Rate
321 Model. Geochem Geophy Geosy 15 (10):3849-3889. doi:10.1002/2014gc005407

322 Matsu'ura R, Nakamura M, Kayano I, Kuarakama I (2003) Short Report on Estimation
323 of Source Regions and Magnitudes of Hyuga-nada Earthquakes in 1662 and 1769,
324 Zenko-ji Earthquake in 1847 and Miyagi Earthquake in 1861 from Intensity Information
325 in Historical Documents. Historical Earthquakes 19:53-61

326 Mochizuki K, Yamada T, Shinohara M, Yamanaka Y, Kanazawa T (2008) Weak
327 interplate coupling by seamounts and repeating M approximately 7 earthquakes.
328 Science 321 (5893):1194-1197. doi:10.1126/science.1160250

329 Nakanishi A, Takahashi N, Yamamoto Y, Takahashi T, Ozgur Citak S, Nakamura T,
330 Obana K, Kodaira S, Kaneda Y (2018) Three-dimensional plate geometry and P-wave
331 velocity models of the subduction zone in SW Japan: Implications for seismogenesis.
332 In: Byrne T, Underwood MB, III, Fisher D et al. (eds) Geology and Tectonics of
333 Subduction Zones: A Tribute to Gaku Kimura, vol 534. Special Paper of the Geological
334 Society of America. doi:10.1130/2018.2534(04)

335 Nishikawa T, Matsuzawa T, Ohta K, Uchida N, Nishimura T, Ide S (2019) The slow
336 earthquake spectrum in the Japan Trench illuminated by the S-net seafloor observatories.
337 Science 365 (6455):808-813. doi:10.1126/science.aax5618

338 Niwa M, Kamataki T, Kurosawa H, Saito‐Kokubu Y, Ikuta M (2020) Seismic
339 subsidence near the source region of the 1662 Kanbun Hyuganada Sea earthquake:
340 Geochemical, stratigraphical, chronological, and paleontological evidences in Miyazaki
341 Plain, southwest Japan. Island Arc 29 (1):e12341. doi:10.1111/iar.12341

342 Obara K, Ito Y (2005) Very low frequency earthquakes excited by the 2004 off the Kii
343 peninsula earthquakes: A dynamic deformation process in the large accretionary prism.
344 Earth Planets Space 57 (4):321-326. doi:10.1186/Bf03352570

345 Obara K, Kato A (2016) Connecting slow earthquakes to huge earthquakes. Science 353
346 (6296):253-257. doi:10.1126/science.aaf1512

347 Okada Y (1992) Internal Deformation Due to Shear and Tensile Faults in a Half-Space.
348 Bull Seismol Soc Am 82 (2):1018-1040

349 Ozawa S (2017) Long-term slow slip events along the Nankai trough subduction zone

after the 2011 Tohoku earthquake in Japan. Earth Planets Space 69 (1):56. doi:10.1186/s40623-017-0640-4

Rolandone F, Nocquet J-M, Mothes PA, Jarrin P, Vallée M, Cubas N, Hernandez S, Plain M, Vaca S, Font Y (2018) Areas prone to slow slip events impede earthquake rupture propagation and promote afterslip. Sci Adv 4 (1):eaao6596. doi:10.1126/sciadv.aao6596

Ruiz S, Metois M, Fuenzalida A, Ruiz J, Leyton F, Grandin R, Vigny C, Madariaga R, Campos J (2014) Intense foreshocks and a slow slip event preceded the 2014 Iquique Mw 8.1 earthquake. Science 345 (6201):1165-1169. doi:10.1126/science.1256074

Takagi R, Uchida N, Obara K (2019) Along-Strike Variation and Migration of Long-Term Slow Slip Events in the Western Nankai Subduction Zone, Japan. J Geophys Res 124 (4):3853-3880. doi:10.1029/2018jb016738

Tanioka Y, Satake K (1996) Tsunami generation by horizontal displacement of ocean bottom. Geophys Res Lett 23 (8):861-864. doi:10.1029/96gl00736

Tsuji Y, Iwase H, Matsuoka Y, Odakiri M, Sato M, Haga Y, Imamura F (2018)

365 Distributions of the heights of the Historical Tsunamis hit the east coast of Kyushu.
366 Research report of tsunami engineering 35:127-170

367 Uchida N, Iinuma T, Nadeau RM, Burgmann R, Hino R (2016) Periodic slow slip
368 triggers megathrust zone earthquakes in northeastern Japan. Science 351
369 (6272):488-492. doi:10.1126/science.aad3108

370 Uchida N, Matsuzawa T (2013) Pre- and postseismic slow slip surrounding the 2011
371 Tohoku-oki earthquake rupture. Earth Planet Sci Lett 374:81-91.
372 doi:10.1016/j.epsl.2013.05.021

373 Usami T (2003) Materials for comprehensive list of destructive earthquakes in Japan.
374 University of Tokyo Press, Tokyo

375 Utsu T (1999) Seismicity Studies: A Comprehensive Review. University of Tokyo Press,
376 Tokyo

377 Wallace LM, Webb SC, Ito Y, Mochizuki K, Hino R, Henrys S, Schwartz SY, Sheehan
378 AF (2016) Slow slip near the trench at the Hikurangi subduction zone, New Zealand.
379 Science 352 (6286):701-704. doi:10.1126/science.aaf2349

380 Wang KL, Bilek SL (2014) Invited review paper: Fault creep caused by subduction of
381 rough seafloor relief. Tectonophysics 610:1-24. doi:10.1016/j.tecto.2013.11.024

382 Wessel P, Smith WHF (1998) New, improved version of generic mapping tools released.
383 Eos Trans AGU 79 (47):579-579. doi:10.1029/98eo00426

384 Yagi Y, Kikuchi M, Sagiya T (2001) Co-seismic slip, post-seismic slip, and aftershocks
385 associated with two large earthquakes in 1996 in Hyuga-nada, Japan. Earth Planets
386 Space 53 (8):793-803. doi:10.1186/Bf03351677

387 Yagi Y, Kikuchi M, Yoshida S, Sagiya T (1999) Comparison of the coseismic rupture
388 with the aftershock distribution in the Hyuga-nada earthquakes of 1996. Geophys Res
389 Lett 26 (20):3161-3164. doi:Doi 10.1029/1999gl005340

390 Yagi Y, Kikuchi M, Yoshida S, Yamanaka Y (1998) Source Process of the Hyuga-nada
391 Earthquake of April 1, 1968 (MJMA 7.5), and its Relationship to the Subsequent
392 Seismicity. Zisin2 51 (1):139-148. doi:10.4294/zisin1948.51.1_139

393 Yamamoto Y, Obana K, Takahashi T, Nakanishi A, Kodaira S, Kaneda Y (2013)
394 Imaging of the subducted Kyushu-Palau Ridge in the Hyuga-nada region, western

395 Nankai Trough subduction zone. Tectonophysics 589:90-102.
396 doi:10.1016/j.tecto.2012.12.028

397 Yamanaka Y, Kikuchi M (2004) Asperity map along the subduction zone in northeastern
398 Japan inferred from regional seismic data. J Geophys Res 109 (B7):B07307.
399 doi:10.1029/2003jb002683

400 Yamashita Y, Shimizu H, Goto K (2012) Small repeating earthquake activity, interplate
401 quasi-static slip, and interplate coupling in the Hyuga-nada, southwestern Japan
402 subduction zone. Geophys Res Lett 39 (8):L08304. doi:10.1029/2012gl051476

403 Yamashita Y, Yakiwara H, Asano Y, Shimizu H, Uchida K, Hirano S, Umakoshi K,
404 Miyamachi H, Nakamoto M, Fukui M, Kamizono M, Kanehara H, Yamada T,
405 Shinohara M, Obara K (2015) Migrating tremor off southern Kyushu as evidence for
406 slow slip of a shallow subduction interface. Science 348 (6235):676-679.
407 doi:10.1126/science.aaa4242

408 Yarai H, Ozawa S (2013) Quasi-periodic slow slip events in the afterslip area of the
409 1996 Hyuga-nada earthquakes, Japan. J Geophys Res 118 (5):2512-2527.

410 doi:10.1002/jgrb.50161

411

412 **Figure legends**

413 **Figure 1**. Location map (inset) and tectonic setting of the Hyuga-nada region,
414 Southwest Japan. The gray shaded regions show the areas of high coseismic slip (more
415 than 50 cm) of the 1968 Hyuga-nada (M_J 7.5), October 1996 (M_J 6.9), and December
416 1996 (M_J 6.7) earthquakes (Yagi et al., 1999; Yagi et al., 1998). The M7-class interplate
417 earthquakes that were detected by the Japan Meteorological Agency since 1923 are
418 indicated by the red stars. The iso-depths on the plate boundary (Nakanishi et al., 2018)
419 are shown by the dashed purple contours (5-km interval). The black circles indicate the
420 source distribution of shallow low-frequency tremor (Yamashita et al., 2015). The red
421 shaded region denotes the focal area of a long-term slow slip event (L-SSE: more than
422 40 cm of cumulative slip (Takagi et al., 2019)). The convergence direction of the
423 Philippine Sea Plate (Kreemer et al., 2014) is shown by the blue arrow. PHS: Philippine
424 Sea Plate, EU: Eurasian Plate, KPR: Kyushu-Palau Ridge.

425

426 **Figure 2**. Fault locations (rectangular faults) and predicted maximum tsunami heights
427 along the coast of Miyazaki Prefecture for each fault model: (a) this study, (b) this study

428 (only northern segment), (c) Hatori model, (d) Matsu'ura model, and (e) comparison of
429 the tsunami heights between all of the models. The value within each rectangular fault
430 indicates the slip amount in meters. The red and gray circles indicate the observed
431 inundation and runup heights (Hatori, 1985; Tsuji et al., 2018), respectively.
432
433 **Preparing tables**
434 **Table 1**. Fault parameters for the 1662 Hyuga-nada Earthquake that were used in this
435 study.
436

Figures

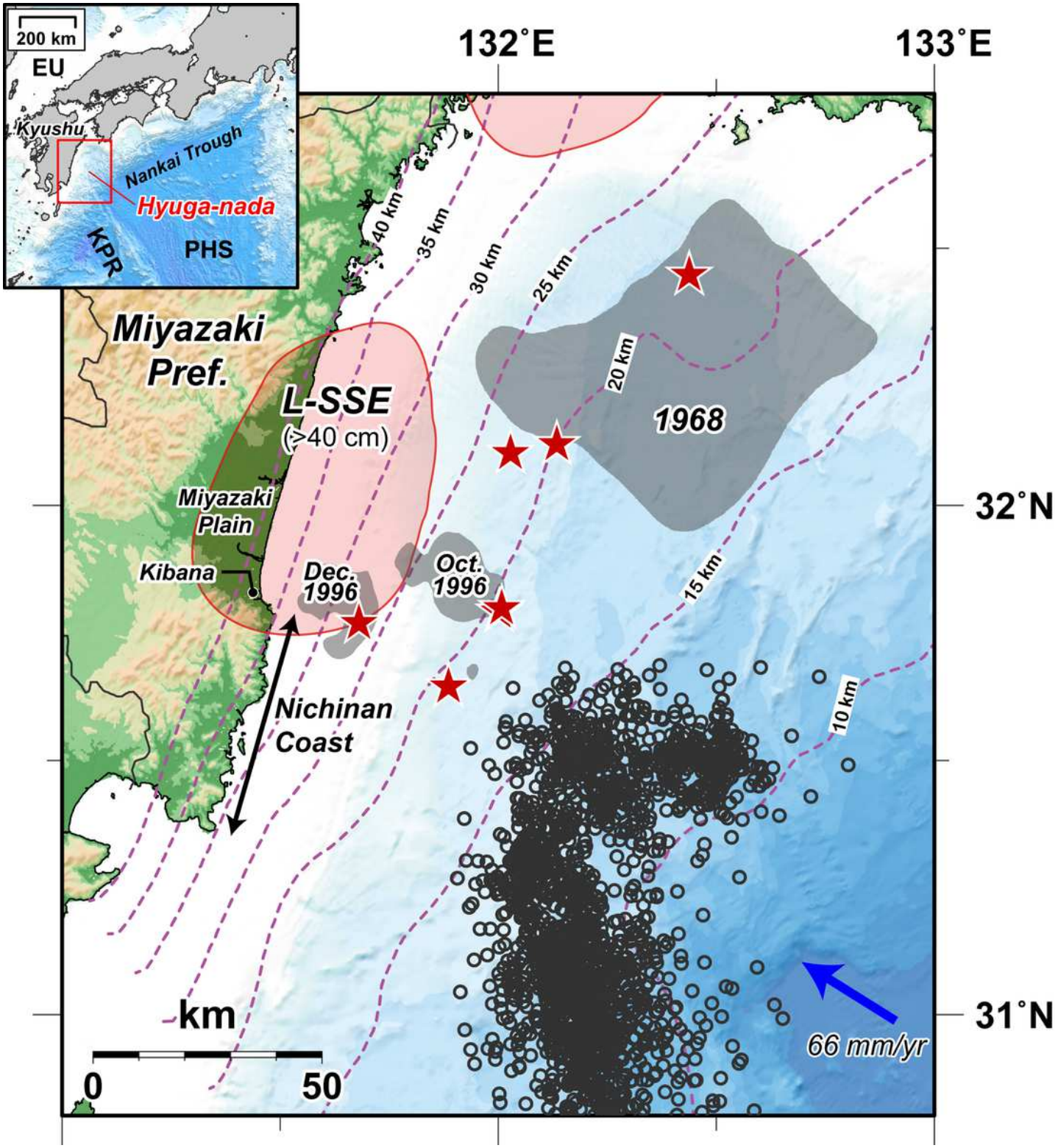

Figure 1

Location map (inset) and tectonic setting of the Hyuga-nada region, Southwest Japan. The gray shaded regions show the areas of high coseismic slip (more than 50 cm) of the 1968 Hyuga-nada (MJ 7.5), October 1996 (MJ 6.9), and December 416 1996 (MJ 6.7) earthquakes (Yagi et al., 1999; Yagi et al.,

1998). The M7-class interplate earthquakes that were detected by the Japan Meteorological Agency since 1923 are indicated by the red stars. The iso-depths on the plate boundary (Nakanishi et al., 2018) are shown by the dashed purple contours (5-km interval). The black circles indicate the source distribution of shallow low-frequency tremor (Yamashita et al., 2015). The red shaded region denotes the focal area of a long-term slow slip event (L-SSE: more than 40 cm of cumulative slip (Takagi et al., 2019)). The convergence direction of the Philippine Sea Plate (Kreemer et al., 2014) is shown by the blue arrow. PHS: Philippine Sea Plate, EU: Eurasian Plate, KPR: Kyushu-Palau Ridge.

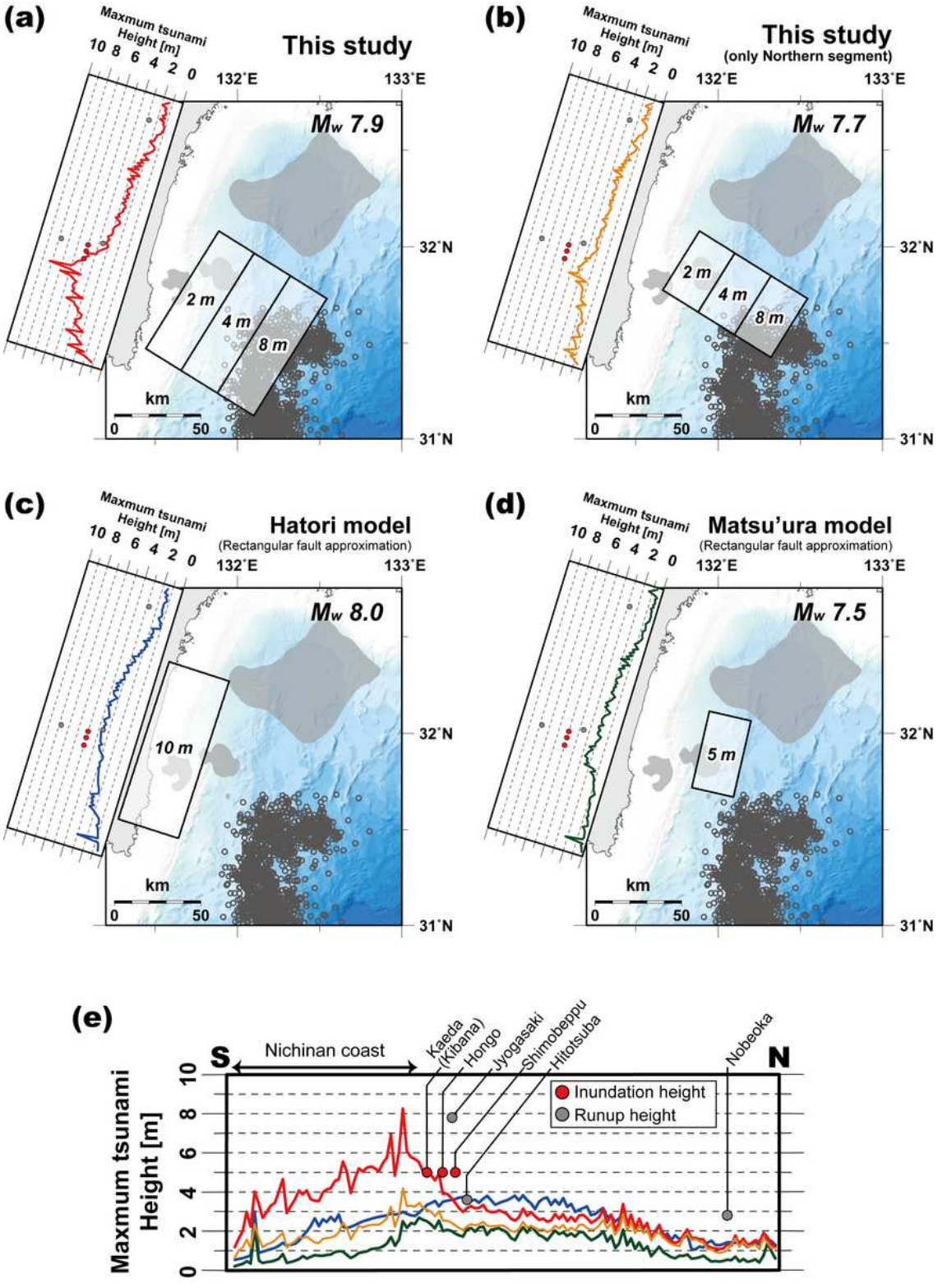

Figure 2

Fault locations (rectangular faults) and predicted maximum tsunami heights along the coast of Miyazaki Prefecture for each fault model: (a) this study, (b) this study (only northern segment), (c) Hatori model, (d) Matsu'ura model, and (e) comparison of the tsunami heights between all of the models. The value within each rectangular fault indicates the slip amount in meters. The red and gray circles indicate the observed inundation and runup heights (Hatori, 1985; Tsuji et al., 2018), respectively.

Supplementary Files

This is a list of supplementary files associated with this preprint. Click to download.

- graphicalabstract.png
- subimttable.pdf